

1 Supporting information

2 Harvesting electricity from benzene and ammonium-contaminated groundwater using a
3 microbial fuel cell with an aerated cathode

4 Manman Wei,^{ab} Falk Harnisch,^c Carsten Vogt,^{*a} Jörg Ahlheim,^d Thomas R. Neu,^e Hans H.
5 Richnow^a

6

7

8

9 ^a Department of Isotope Biogeochemistry, Helmholtz Centre for Environmental Research - UFZ,
10 Permoserstraße 15, 04318 Leipzig, Germany

11 ^b Faculty of Natural Sciences, Hohenheim University, 70593 Stuttgart, Germany

12 ^c Department of Environmental Microbiology, Helmholtz Centre for Environmental Research -
13 UFZ, Permoserstraße 15, 04318 Leipzig, Germany

14 ^d Department of Groundwater Remediation, Helmholtz Centre for Environmental Research -
15 UFZ, Permoserstraße 15, 04318 Leipzig, Germany

16 ^e Department of River Ecology, Helmholtz Centre for Environmental Research - UFZ,
17 Brueckstrasse 3A, 39114, Magdeburg, Germany

18

19 Summary:

20 Page S2: Figure S1

21 Page S3: Figure S2

22 Page S4: Figure S3

23 Page S5: Figure S4

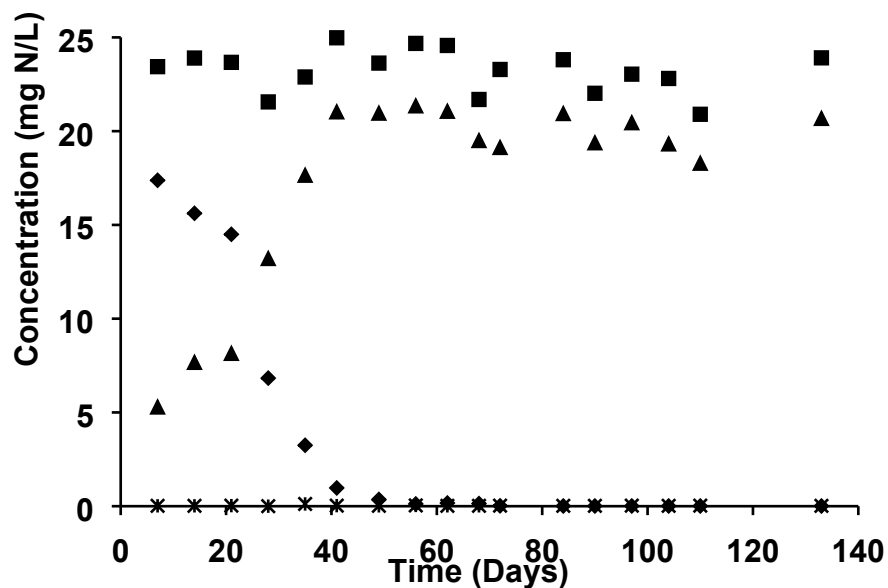
24 Page S7: Figure S5

25

26 Results

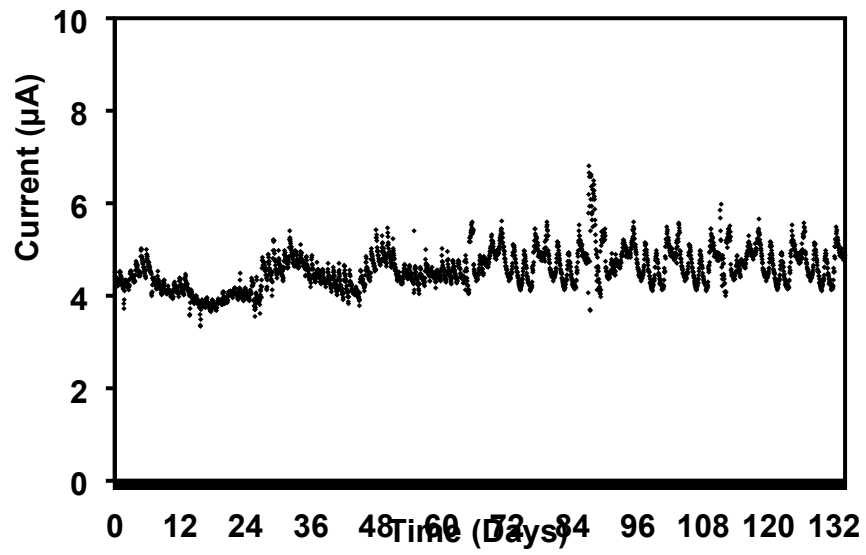
27 Observation of biofilm formation and morphology

28 Biofilm formation in MFCs can be critical for extracellular electron transfer and stable power
29 generation.^{1, 2} A high density of microorganisms with different morphologies was observed and
30 the biofilms appeared to be closely associated with the graphite surface. There was no
31 fundamental difference between biofilms developed in the two compartments of the control
32 reactor, supporting the hypothesis that it was a homogenous mesocosm. At the cathode of the
33 MFC, many rod-shaped cells clustered to form a lot of filaments, which was significantly
34 different from the cell morphology of the biofilms observed at the anode of the MFC, indicating
35 complex microbial community.



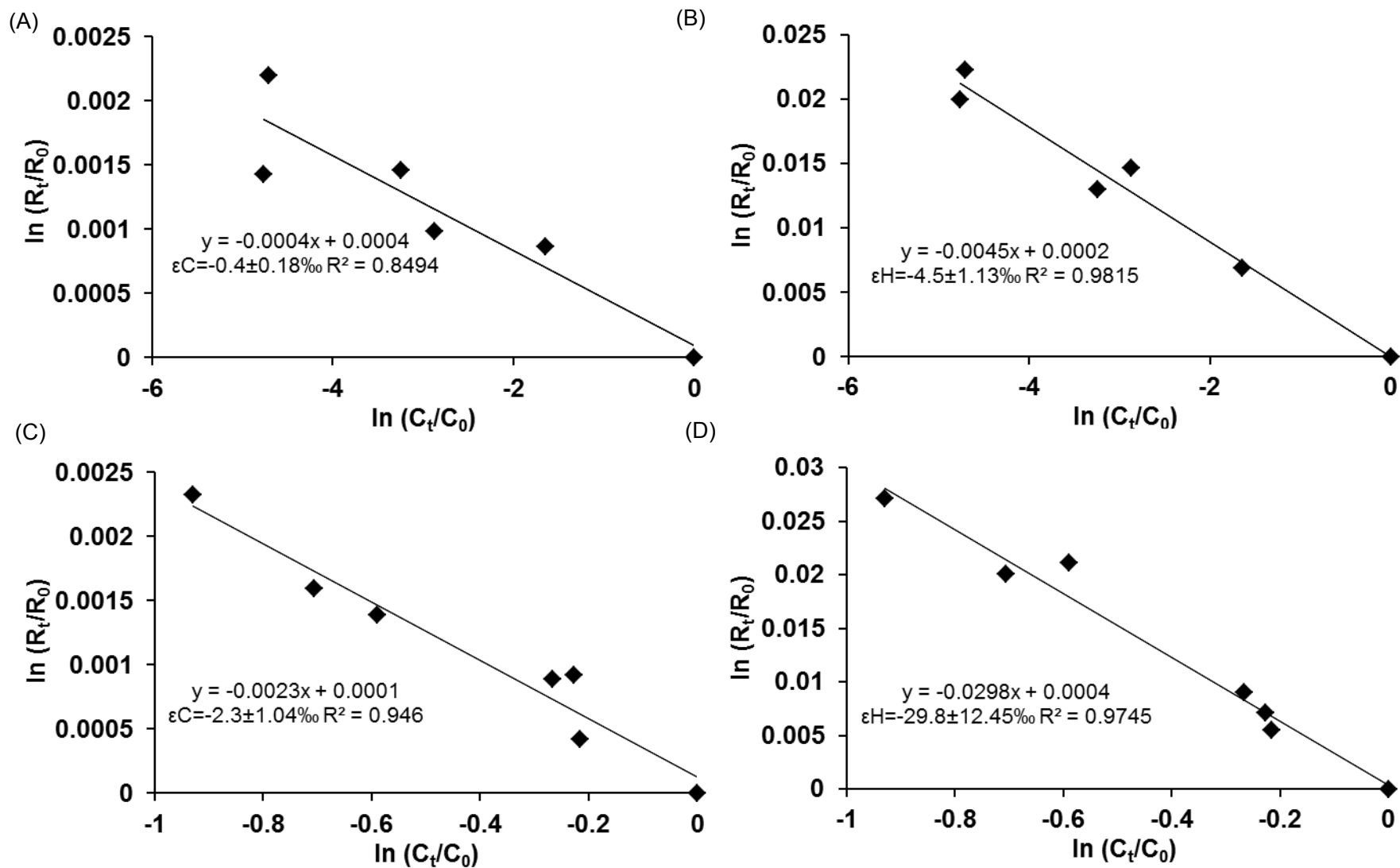
36

37 **Figure S1.** Concentration changes of NH₄⁺, NO₂⁻, and NO₃⁻ in the cathodic compartment of the
38 MFC during continuous treatment. Influent NH₄⁺-N (■), Effluent NH₄⁺-N (◆), Effluent NO₂⁻-
39 N (*), Effluent NO₃⁻-N (▲).



40

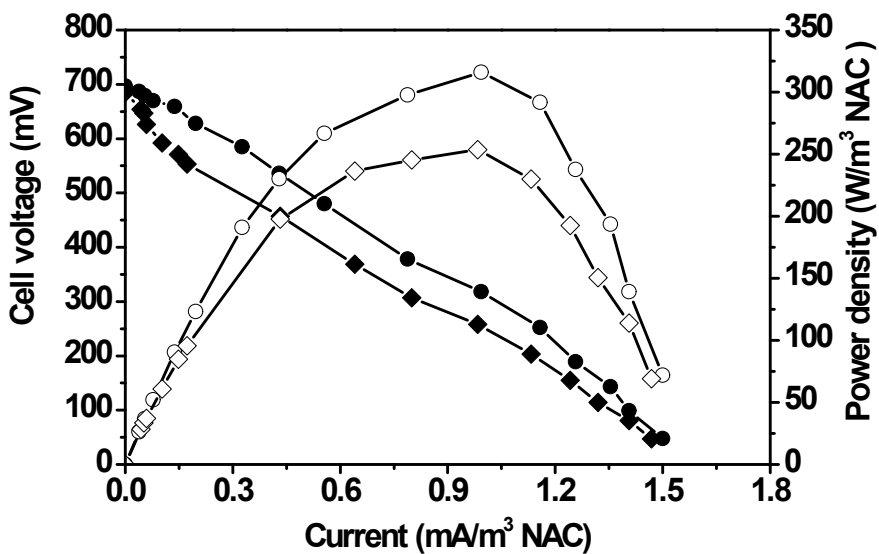
41 **Figure S2.** Noise current observed in the control during continuous treatment of contaminated
42 groundwater.



43
 44 **Figure S3.** Rayleigh plot for carbon and hydrogen stable isotope fractionation of the anodic benzene in the MFC and the control

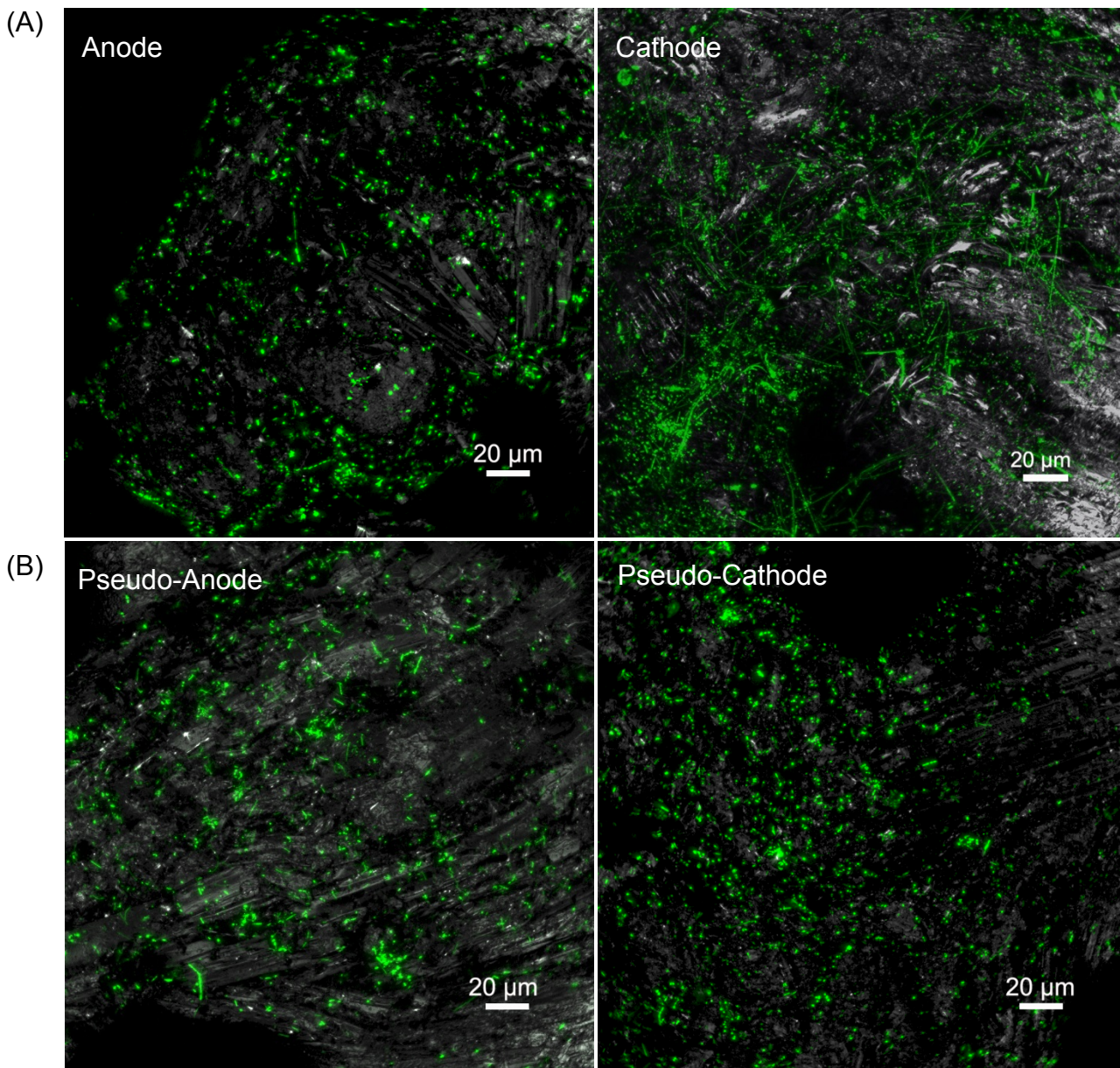
45 reactor. The lines correspond to a linear regression: carbon (A) and hydrogen (B) isotope fractionation in the MFC; carbon (C) and

46 hydrogen (D) isotope fractionation in the Control. C_0 : the benzene concentration at the influent; C_t : the benzene concentration at the
47 anodic effluent; R_0 : the isotope ratio determined at the influent; R_t : the isotope ratio at the anodic effluent. Enrichment factors (ϵ) are
48 given with the uncertainty (\pm confidence interval 95%).



49

50 **Figure S4.** Forwards (circle symbol) and backwards (diamond symbol) polarization and power
 51 density curves of the MFC at a flow rate of 0.3 mL/min. Solid symbols represent cell voltage;
 52 open symbols represent power density. Polarization and power curves usually do not overlap
 53 when resistors are switched in forward (from high to low) and backward (from low to high)
 54 orders. In our study, a slight hysteresis was observed between the forward and backward curves.
 55 The backward polarization curve is below the forward one with a difference of ~50 mV.



56

57 **Fig. S5** Confocal laser scanning microscopy (CLSM) of biofilms colonizing the surface of
 58 granular graphite in the MFC (A) and control (B). Data sets are shown as maximum intensity
 59 projection. Please take notice of the morphological diversity of bacteria at the cathode (A). Color
 60 allocation: reflection–white, nucleic acid stain–green.

61 **References**

- 62 1. L. Zhang, X. Zhu, J. Li, Q. Liao and D. D. Ye, *J. Power Sources*, 2011, **196**, 6029-6035.
 63 2. K. Chung, I. Fujiki and S. Okabe, *Bioresour. Technol.*, 2011, **102**, 355-360.

64